JOURNAL OF
GYNECOLOGIC
ONCOLOGY

Original Article

Check for updates

Circular RNA intraflagellar transport 80 facilitates endometrial cancer progression through modulating miR-545-3p/FAM98A signaling

Na Wang (ID),[1] **Yunfeng Guo** (ID),[2] **Liqin Song** (ID),[3] **Tong Tong** (ID),[4] **Xiaomei Fan** (ID)[2]

[1]Department of Obstetrics and Gynecology, The Fourth Hospital of Hebei Medical University, Shijiazhuang, Hebei, China
[2]Department of Gynecological Oncology, The Fourth Hospital of Hebei Medical University, Shijiazhuang, Hebei, China
[3]Department of Obstetrics and Gynecology, Longyao County Hospital, Longyao, Hebei, China
[4]Department of Anesthesiology, The Fourth Hospital of Hebei Medical University, Shijiazhuang, Hebei, China

OPEN ACCESS

Correspondence to
Xiaomei Fan
Department of Gynecological Oncology, The Fourth Hospital of Hebei Medical University, No. 12, JianKang Road, Shijianzhuang, Hebei 050011, China.
E-mail: fanxiaomei2006@163.com

ORCID iDs
Na Wang (ID)
https://orcid.org/0000-0002-7838-170X
Yunfeng Guo (ID)
https://orcid.org/0000-0002-0705-3629
Liqin Song (ID)
https://orcid.org/0000-0002-9678-4449
Tong Tong (ID)
https://orcid.org/0000-0002-5015-1670
Xiaomei Fan (ID)
https://orcid.org/0000-0003-3035-876X

Conflict of Interest
No potential conflict of interest relevant to this article was reported.

ABSTRACT

Objective: Endometrial cancer (ECa) is a common gynecological malignancy. Circular RNAs (circRNAs) have been identified as key regulators of human tumorigenesis and development. Herein, we explored the role and mechanism of circular RNA intraflagellar transport 80 (circ-IFT80, also called circ_0067835) in ECa.

Methods: Circ-IFT80, microRNA-545-3p (miR-545-3p), and family with sequence similarity 98 member A (FAM98A) were quantified by quantitative real-time polymerase chain reaction or Western blot. The biological characteristics of ECa cells were evaluated via Cell Counting Kit-8, 5-ethynyl-2′-deoxyuridine, transwell, tube formation and flow cytometry assays. Dual-luciferase reporter assay or RNA pull-down assay was employed to verify the binding relationship between miR-545-3p and circ-IFT80 or FAM98A. Xenograft assays were conducted to analyze the effect of circ-IFT80 in vivo.

Results: Circ-IFT80 and FAM98A were up-regulated, and miR-545-3p was down-regulated in ECa tissues and cells. Knockdown of circ-IFT80 blocked proliferation, migration, invasion and angiogenesis and promoted apoptosis in ECa cells. Moreover, circ-IFT80 harbored a binding site for miR-545-3p, and the effects of circ-IFT80 were mediated by miR-545-3p. FAM98A was a direct target of miR-545-3p, and miR-545-3p hindered ECa cell progression via targeting FAM98A. Circ-IFT80 induced FAM98A expression through miR-545-3p. Furthermore, silence of circ-IFT80 suppressed tumor growth in vivo.

Conclusion: Circ-IFT80 may promote the malignant progression of ECa cells at least in part by modulating miR-545-3p/FAM98A axis, providing a potential therapeutic target for ECa.

Keywords: Endometrial Cancer; Circular RNA Intraflagellar Transport 80; MicroRNA; Tumor Progression

Generated by xmlinkpress

Author Contributions

Conceptualization: T.T.; Data curation: G.Y., S.L., F.X.; Formal analysis: G.Y., F.X.; Investigation: W.N., S.L., T.T.; Methodology: G.Y., S.L., T.T., F.X.; Resources: G.Y., S.L.; Software: W.N., T.T.; Supervision: W.N.; Validation: W.N.; Writing - original draft: W.N.; Writing - review & editing: F.X.

Synopsis

We further investigated the potential role of circ-IFT80 in endometrial cancer (ECa) and unveiled that circ-IFT80 accelerated the malignant progression of ECa via decoying miR-545-3p and consequently enhancing FAM98A. Our findings provided novel insights into the pathogenesis of ECa and revealed promising therapeutic targets.

INTRODUCTION

Endometrial cancer (ECa) is a frequent malignancy in women, especially in western countries [1]. According to the global cancer statistics in 2020, the number of cases of ECa reached 417,000, ranking sixth in the incidence of female cancer [2]. Moreover, the 5-year overall survival rate of patients with metastatic or recurrent ECa is very low, only 10%–20% [3]. Therefore, exploring novel biomarkers for early diagnosis and treatment of ECa is essential for enhancing the survival rate of patients.

Circular RNAs (circRNAs) are single-stranded RNA molecules generated by the back-splicing process [4,5]. Numerous studies have identified the important regulatory roles of circRNAs in gynecological malignant tumors, including cervical carcinoma [6], ovarian cancer [7] and ECa [8]. Recently, some reports have confirmed that dysregulated circRNAs participate in the pathogenesis of ECa [9]. For example, hsa_circ_0002577 showed increased expression in ECa, and its depletion impeded the viability and mobility of ECa cells [10]. Circ_0001776 was down-regulated in ECa, and its elevation hindered ECa cell proliferation and glycolysis [11]. Interestingly, circular RNA intraflagellar transport 80 (circ-IFT80; also called circ_0067835), derived from the back-spliced exons of intraflagellar transport 80 (IFT80) mRNA, was conspicuously increased in ECa and exerted a carcinogenic effect on ECa [12]. Nonetheless, our understanding of its molecular determinants in ECa is still limited.

Emerging investigations have confirmed that circRNAs participate in cancer progression by functioning as competing endogenous RNAs (ceRNAs) or microRNA (miRNA) sponges [13,14]. For instance, circ_0109046 contributed to the malignant progression of ECa by up-regulating HMGA2 through binding to miR-136 [15]. Aberrantly expressed miRNAs have been reported in ECa, highlighting their roles as promising targets for the prognosis and treatment of ECa [16,17]. Up-regulation of miR-93-5p facilitated ECa metastasis through regulating IFNAR1/STAT3 pathway [18]. Also, miR-1271 hampered the malignant behaviors of ECa via binding to LDHA [19]. A previous research revealed a significant reduction in miR-545-3p in ECa [20]. However, the connection between circ-IFT80 and miR-545-3p in ECa remains indistinct.

In the present research, we validated the oncogenic function of circ-IFT80 in ECa. Furthermore, we first uncovered a novel circ-IFT80/miR-545-3p/family with sequence similarity 98 member A (FAM98A) axis in ECa.

MATERIALS AND METHODS

1. Specimen collection

ECa tissues (n=35) and matched normal tissues (n=35) were collected from 35 ECa patients undergoing surgery at The Fourth Hospital of Hebei Medical University. The clinical features of these patients were provided in Table S1. All participators signed written informed consent. The exclusion criteria of this study are: receiving any radiotherapy or chemotherapy. This study was approved by the Ethics Committee of The Fourth Hospital of Hebei Medical University (IRB No. 2019HBZ551).

2. Cell culture and transfection

Human ECa cells (HEC-1B, EEC and Ishikawa) and normal endometrial epithelial cells (human embryonic stem cell [hESC]) were commercially acquired from Tongpai Biotech (Shanghai, China) and incubated in RPMI-1640 medium (Procell, Wuhan, China) supplemented with 10% fetal bovine serum (FBS; Procell). All cells were cultivated in a humidified incubator with 5% CO_2 at 37°C.

Circ-IFT80 siRNA (si-circ-IFT80), miR-545-3p mimics (miR-545-3p), miR-545-3p inhibitor (anti-miR-545-3p), and corresponding negative controls (si-NC, miR-NC and anti-miR-NC) were provided by Ribobio (Guangzhou, China). To achieve overexpression, the full-length sequence of circ-IFT80 or the coding region of FAM98A was inserted into pCD5-ciR vector (Geneseed, Guangzhou, China) or pcDNA3.1 vector (Youbio, Hunan, China), respectively. Additionally, 50 nM oligonucleotides or 2 μg plasmids were introduced into ECa cells utilizing Lipofectamine™ 3000 (Invitrogen, Carlsbad, CA, USA) following the manufacturer's requirements.

3. Quantitative real-time polymerase chain reaction (qRT-PCR)

HEC-1B and Ishikawa cells were fractionated into nucleus fraction and cytoplasm fraction using the Nuclear/Cytosol Fractionation Kit (Biovision, San Francisco Bay, CA, USA). RNA was extracted with the TRIzol reagent (Leagene, Beijing, China). For RNase R digestion, 2 μg of RNA was exposed to RNase R (Seebio, Shanghai, China) for 20 minutes at 37°C. Complementary DNA (cDNA) was generated from RNA using the specific cDNA synthesis kit (Vazyme, Nanjing, China). qRT-PCR was performed using SYBR Green Master Mix (Vazyme) with gene-specific primer pairs. U6 or glyceraldehyde 3-phosphate dehydrogenase (GAPDH) served as an endogenous reference. All primers were shown: circ-IFT80-F: 5′-CCGCCCACTGTACAATTCAC-3′, circ-IFT80-R: 5′-CAGTAGTCCAGCCCACACAG-3′; IFT80-F: 5′-GCAAGGAACACCAGTGTATTCA-3′, IFT80-R: 5′-GGCCGTAACTATCCCATACCTTA-3′; miR-545-3p-F: 5′-GCCGAGTCAGCAAACA TTTA-3′, miR-545-3p-R: 5′-CAGTGCAGGGTCCGAGGTAT-3′; FAM98A-F: 5′-CTTGAGGTGA GTGGGCTACTA-3′, FAM98A-R: 5′-TGAGGTATGTGAGCAAGAGGAG-3′; U6-F: 5′-CTCGCTT CGGCAGCACATA-3′, U6-R: 5′-AACGCTTCACGAATTTGCGT-3′; GAPDH-F: 5′-GGAGCGAG ATCCCTCCAAAAT-3′, GAPDH-R: 5′-GGCTGTTGTCATACTTCTCATGG-3′.

4. Cell Counting Kit-8 (CCK-8) assay

HEC-1B and Ishikawa cells in 96-well plates were cultivated at 37°C for 48 hours following transfection. After that, 10 μL of CCK-8 (Beyotime, Shanghai, China) was added in each well. After 4 hours incubation, the absorbance was examined using a microplate reader (Bio-Rad, Hercules, CA, USA).

5. 5-Ethynyl-2′-deoxyuridine (EdU) assay

According to the manufacturer's recommendations, the BeyoClick EdU Cell Proliferation Kit (Beyotime) was employed to determine the proliferation capacity of ECa cells. Fluorescence microscope (Olympus, Tokyo, Japan) was utilized to count EdU positive cells.

6. Transwell assay

The invasion and migration abilities of ECa cells were determined utilizing transwell inserts (Corning, Corning, NY, USA) pre-coated with (invasion assay) or without (migration assay) Matrigel (Corning). The upper chamber was filled with HEC-1B and Ishikawa cells. Simultaneously, 10% FBS (Procell) was dropped into the bottom chamber. Twenty-four hours later, the invaded or migrated cells were counted under a microscope (Olympus; magnification: 100×) after crystal violet staining.

7. Tube formation assay

$2.5×10^4$ HUVECs (Tongpai Biotech) were cultivated in the conditioned medium of transfected HEC-1B and Ishikawa cells on 24-well plates pre-coated with Matrigel (Corning). Afterwards, angiogenesis was assessed via examining the number of branches under a microscope (Olympus).

8. Flow cytometry

Following different transfections, HEC-1B and Ishikawa cells were harvested and trypsinized. After the pellets were resuspended with phosphate buffer saline (PBS; Solarbio, Beijing, China), cells were treated sequentially with RNase A (Solarbio) and propidium iodide (PI; Abcam, Cambridge, UK). Finally, a flow cytometer (Beckman Coulter, Miami, FL, USA) was used to monitor cell cycle distribution.

Cell apoptosis was determined utilizing the Annexin V-FITC/PI Apoptosis Detection kit (Yeasen, Shanghai, China) following the manufacturer's requirements. The apoptosis rates of HEC-1B and Ishikawa cells were tested utilizing a flow cytometer (Beckman Coulter).

9. Western blot assay

The protein was extracted utilizing the RIPA buffer (Beyotime). After be separated by 10% sodium dodecyl sulfate-polyacrylamide gel electrophoresis, the protein was blotted onto polyvinylidene fluoride membranes (Beyotime). Afterwards, the membranes were probed with primary antibodies, including anti-proliferating cell nuclear antigen (PCNA) (1:1,000, ab18197; Abcam), anti-B-cell lymphoma-2 (Bcl-2) (1:500, ab59348; Abcam), anti-Bcl-2 associated X protein (Bax) (1:2,000, ab182733; Abcam), anti-FAM98A (1:2,000, ab204083; Abcam) and anti-GAPDH (1:2,500, ab9485; Abcam). The protein bands were observed through ECL system (Beyotime) after incubating with the secondary antibody (1:20,000, ab205718; Abcam).

10. Bioinformatics

Online prediction tool circinteractome was used to search the miRNAs that potentially bind to circ-IFT80 at https://circinteractome.nia.nih.gov/. The miRNA-binding sites to human 3'UTRs were predicted using the prediction database starBase at http://starbase.sysu.edu.cn/.

11. RNA pull-down assay

For this assay, a mix of Biotin-labeled circ-IFT80 probe or the nontarget sequence control (oligo probe) and M-280 Streptavidin Dynabeads (Invitrogen) was prepared at 37°C for 2

hours. Then, HEC-1B and Ishikawa cells were lysed in RIPA buffer, and the lysates were incubated with probe-coated beads for 3 hours at 4°C. The abundance of RNAs was measured by qRT-PCR assay.

12. Dual-luciferase reporter assay

The wild-type reporter (WT-circ-IFT80 or WT-FAM98A 3'UTR) and mutant reporter (MUT-circ-IFT80 or MUT-FAM98A 3'UTR) were synthesized by Ribobio. The appropriate reporter was introduced into ECa cells together with miR-545-3p mimic or miR-NC mimic. Forty-eight hours later, a Dual-Lucy Assay Kit (Solarbio) was employed to examine the luciferase intensity.

13. In vivo assay

This assay was approved by the Research Ethics Committee of The Fourth Hospital of Hebei Medical University. Ten BALB/c nude mice aged 5 weeks were equally divided into 2 groups (n=5 per group). Lentivirus expressing circ-IFT80 shRNA (sh-circ-IFT80) or the control (sh-NC), purchased from Ribobio, were introduced into Ishikawa cells. Afterwards, 1×10^7 Ishikawa cells were subcutaneously injected into the back of nude mice. Subsequently, tumor volume was monitored every 7 days and calculated by the following formula: Volume (mm³)=(width²×length)/2. After 28 days, the excised xenograft tumors were used for weight and RNA expression analysis.

14. Immunohistochemistry (IHC)

Formalin-fixed, paraffin-embedded xenograft tumors were sectioned at 5 μm. Following dewaxing and rehydration, the sections were treated with CPBS buffer (Solarbio) for antigen restoration. After washing with PBS (Solarbio) and blocking with 10% goat serum (Abcam), the sections were probed with anti-Ki67 antibody (ab21700; Abcam), followed by incubation with a secondary antibody (ab205718; Abcam). Then, the sections were counterstained with hematoxylin (Solarbio) after staining with DAB (Leagene). Finally, the sections were observed using a microscope (Olympus) after sealing with neutral resin (Solarbio).

15. Statistical analysis

Data were acquired from 3 independent experiments and displayed as mean±standard deviation. The difference was determined using a Student's t-test and one-way analysis of variance by GraphPad Prism 7 software (GraphPad, San Diego, CA, USA). Statistical significance was identified when p<0.05. Correlation between circ-IFT80 or miR-545-3p expression and clinical features of these patients was determined by χ^2 test. For variable expression correlation in ECa tissues, Pearson's correlation coefficients were used.

RESULTS

1. Circ-IFT80 level is boosted in ECa tissues and cell lines

Firstly, we utilized qRT-PCR to detect the expression pattern of circ-IFT80 in ECa tissues and normal tissues. As displayed in **Fig. 1A**, circ-IFT80 level was prominently increased in ECa tissues compared to normal tissues. Additionally, ECa patients were divided into 2 groups according to tumor, node, metastasis (TNM) staging, and qRT-PCR analysis showed that circ-IFT80 level in tumor tissues of ECa patients in stage III (n=22) was remarkably higher than that in stage I–II (n=13) (**Fig. 1B**). Moreover, circ-IFT80 level showed a significant increase in ECa cells (HEC-1B, EEC and Ishikawa) compared to normal hESCs (**Fig. 1C**). The schematic diagram displayed that circ-IFT80 is derived from exons 4 to 9 of IFT80 mRNA (**Fig. 1D**).
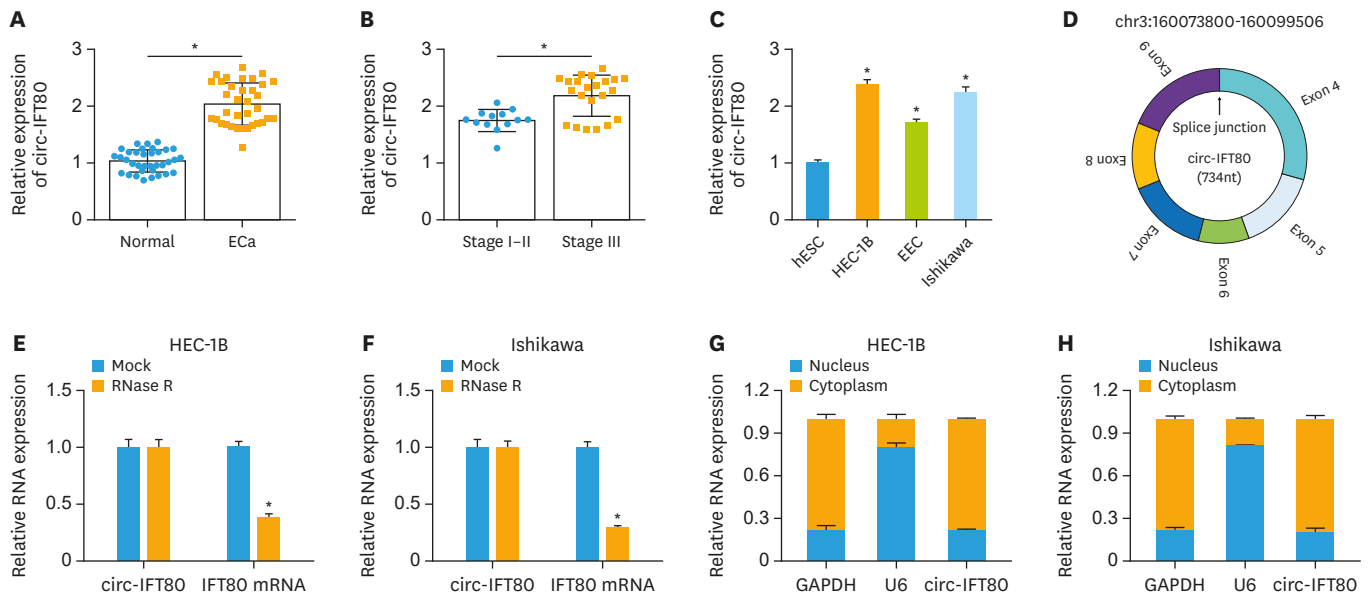
Fig. 1. Expression of circ-IFT80 in ECa. (A) Circ-IFT80 level in ECa tissues (n=35) and matched normal tissues (n=35) was detected using qRT-PCR. (B) According to TNM staging, ECa patients were divided into 2 groups, and circ-IFT80 level was checked by qRT-PCR. (C) Circ-IFT80 level in ECa cells (HEC-1B, EEC and Ishikawa) and hESCs was examined using qRT-PCR. (D) The schematic diagram exhibited the cyclization of circ-IFT80. (E, F) RNA of HEC-1B and Ishikawa cells was incubated with RNase R and then the levels of circ-IFT80 and IFT80 mRNA were tested using qRT-PCR. (G, H) The distribution of circ-IFT80 in HEC-1B and Ishikawa cells was determined by qRT-PCR.

circ-IFT80, circular RNA intraflagellar transport 80; ECa, endometrial cancer; GAPDH, glyceraldehyde 3-phosphate dehydrogenase; hESC, human embryonic stem cell; IFT80, intraflagellar transport 80; qRT-PCR, quantitative real-time polymerase chain reaction; TNM, tumor, node, metastasis.
*$p<0.05$.

Following RNase R treatment, qRT-PCR analysis revealed that circ-IFT80 was resistant to RNase R compared with IFT80 linear mRNA (**Fig. 1E and F**). Furthermore, subcellular localization assay showed that circ-IFT80 was mainly present in the cytoplasm of ECa cells (**Fig. 1G and H**). Additionally, circ-IFT80 expression was closely correlated with the TNM stage, histological grade, myometrial invasion, and lymphatic metastasis of the tumors (**Table S1**). Taken together, circ-IFT80 is overexpressed in human ECa.

2. Silence of circ-IFT80 inhibits proliferation, migration, invasion and angiogenesis and triggers apoptosis in ECa cells

To study the potential function of circ-IFT80 in ECa, loss-of-function experiments were carried out by transfecting si-circ-IFT80 into HEC-1B and Ishikawa cells. qRT-PCR results revealed that transfection of si-circ-IFT80 significantly reduced the expression of circ-IFT80, not IFT80 linear mRNA level (**Fig. 2A and B**). CCK-8 and EdU assays showed that suppression of circ-IFT80 markedly reduced the proliferative ability of ECa cells (**Fig. 2C and E**). Transwell and tube formation assays showed that depletion of circ-IFT80 strikingly weakened the migration and invasion capabilities of ECa cells and restrained tube formation (**Fig. 2F-H**). Furthermore, flow cytometry revealed that circ-IFT80 silencing induced cell cycle arrest by increasing cells in G0/G1 phase and decreasing cells in S phase (**Fig. 3A**). Also, depletion of circ-IFT80 strikingly promoted the apoptosis of HEC-1B and Ishikawa cells (**Fig. 3B**). Western blot assay was utilized to detect protein levels related to proliferation and apoptosis. As shown in **Fig. 3C and D**, down-regulation of circ-IFT80 resulted in a striking decrease in PCNA and Bcl-2 levels and a marked elevation in Bax level. Collectively, silencing of circ-IFT80 hindered the malignant progression of ECa cells. Additionally, in normal endometrial epithelial hESCs, overexpression of circ-IFT80 promoted cell proliferation, migration and invasion (**Fig. S1**), supporting the oncogenic role of circ-IFT80 in ECa.
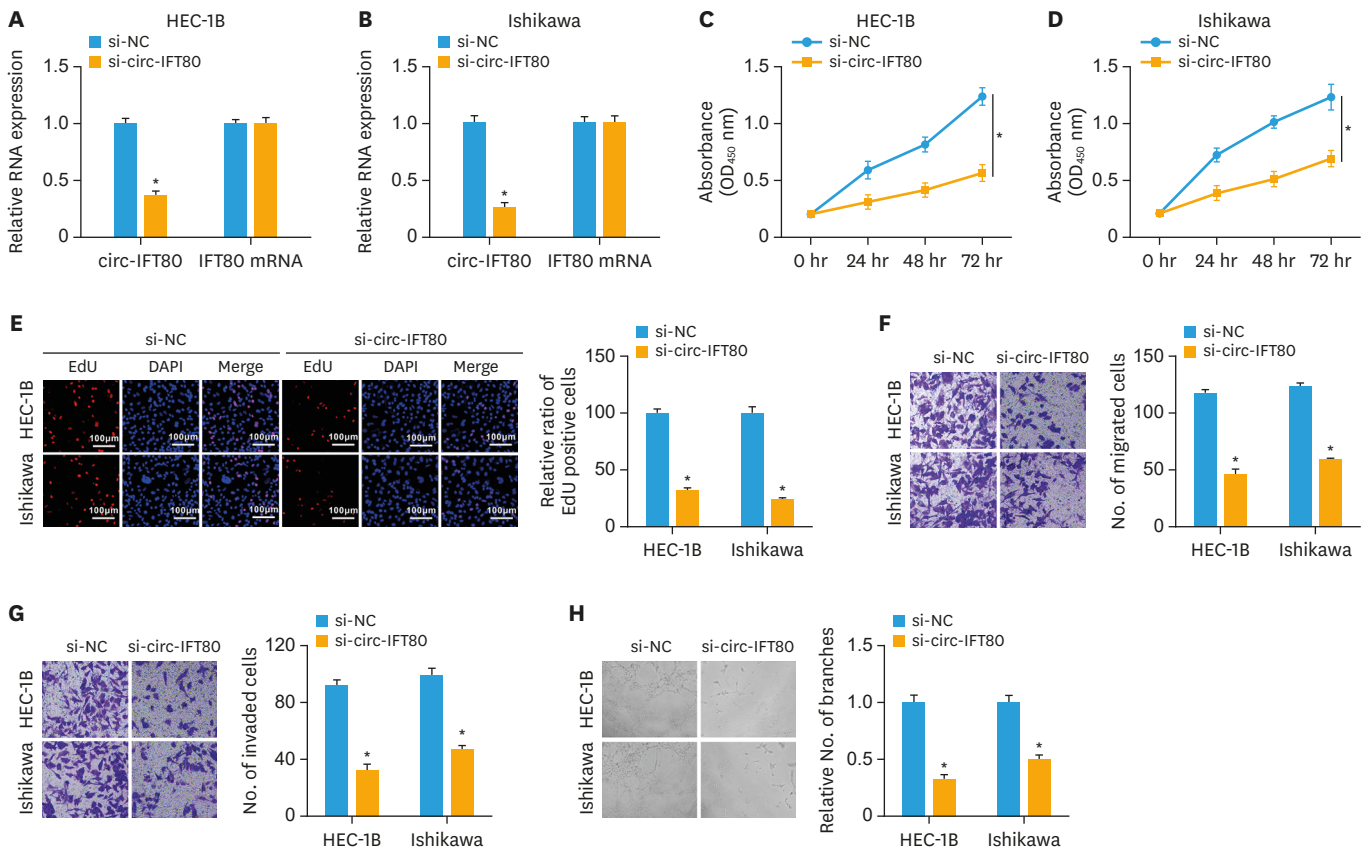
Fig. 2. Effect of circ-IFT80 silence on ECa cells. (A, B) After transfecting si-NC or si-circ-IFT80 into ECa cells, qRT-PCR was utilized to detect the levels of circ-IFT80 and IFT80 mRNA. After transfection, cell proliferation was evaluated by CCK-8 (C, D) and EdU (E) methods. Cell migration (F), invasion (G), and angiogenesis (H) were determined via transwell and tube formation.

CCK-8, Cell Counting Kit-8; circ-IFT80, circular RNA intraflagellar transport 80; DAPI, 4′,6-diamidino-2-phenylindole; ECa, endometrial cancer; EdU, 5-ethynyl-2′-deoxyuridine; IFT80, intraflagellar transport 80; si-circ-IFT80, circular RNA intraflagellar transport 80 siRNA; qRT-PCR, quantitative real-time polymerase chain reaction.

*$p < 0.05$.

3. Circ-IFT80 serves as a sponge for miR-545-3p

Using the circinteractome online software, we selected 8 candidate miRNAs that were associated with ECa progression. RNA pull-down assay exhibited that circ-IFT80 probe had the most significant binding with miR-545-3p in HEC-1B and Ishikawa cells, so miR-545-3p was selected for follow-up research (**Fig. 4A and B**). The potential binding site of circ-IFT80 and miR-545-3p was displayed in **Fig. 4C**. This presumed targeting relationship was confirmed by using dual-luciferase reporter assay. Overexpression of miR-545-3p by miRNA mimic transfection, confirmed by qRT-PCR analysis (**Fig. 4D**), prominently decreased the luciferase activity of WT-circ-IFT80 reporter but not MUT-circ-IFT80 reporter (**Fig. 4E and F**). Then, miR-545-3p level was determined in ECa patients and cells. As exhibited in **Fig. 4G and H**, miR-545-3p expression in ECa tissues and cells was markedly lower than that in normal groups. Interestingly, in ECa tissues, we found a strong inverse correlation between miR-545-3p and circ-IFT80 expression levels (**Fig. S2A**). Additionally, miR-545-3p expression was associated with the TNM stage, histological grade, myometrial invasion, and lymphatic metastasis of the tumors (**Table S2**). Besides, introduction of oe-circ-IFT80 led to a significant increase in circ-IFT80 level (**Fig. 4I**). Knockdown of circ-IFT80 accelerated the expression of miR-545-3p, while overexpression of circ-IFT80 blocked the expression of miR-545-3p (**Fig. 4J and K**). These data together suggested that circ-IFT80 affected miR-545-3p expression in ECa cells.
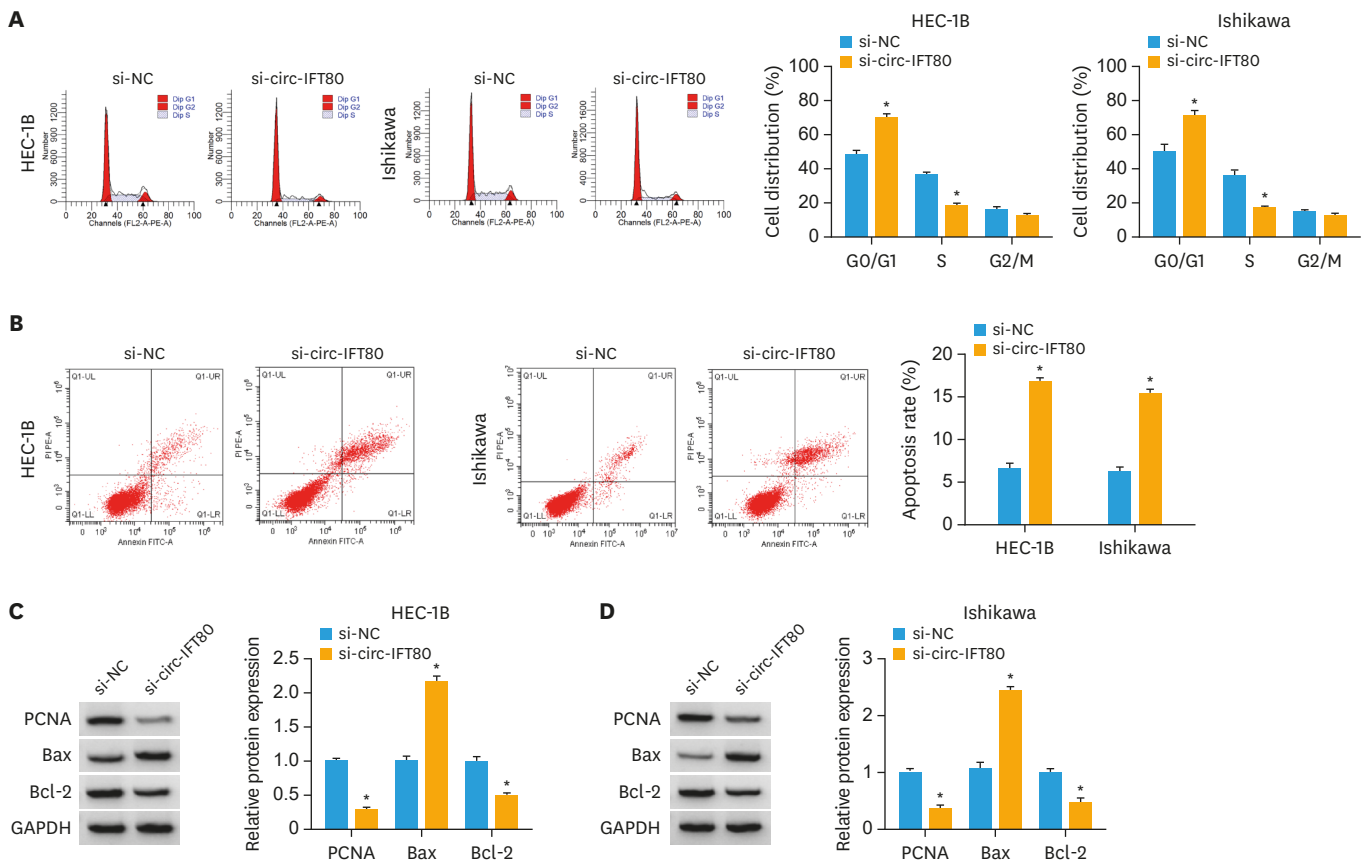
Fig. 3. Effect of circ-IFT80 silence on ECa cells. After transfection, cell cycle distribution (A) and apoptosis (B) were determined by flow cytometry. (C, D) Western blot was employed to examine the levels of proliferation-related protein (PCNA) and apoptosis-related proteins (Bax and Bcl-2).
Bax, B-cell lymphoma-2 associated X protein; Bcl-2, B-cell lymphoma-2; circ-IFT80, circular RNA intraflagellar transport 80; ECa, endometrial cancer; GAPDH, glyceraldehyde 3-phosphate dehydrogenase; PCNA, proliferating cell nuclear antigen; si-circ-IFT80, circular RNA intraflagellar transport 80 siRNA.
*p<0.05.

4. MiR-545-3p directly targets FAM98A

To identify miR-545-3p targets, we used the starBase online software. Among these candidates, we selected several genes that were associated with ECa pathogenesis. Intriguingly, in miR-545-3p-overexpressing HEC-1B and Ishikawa cells, we found that FAM98A mRNA level was the most significantly downregulated among these targets (**Fig. S3A and B**). We thus selected FAM98A for further investigations. Moreover, the starBase online software unveiled that FAM98A 3'UTR harbored a potential binding site for miR-545-3p (**Fig. 5A**). To verify this, dual-luciferase reporter assay was implemented in HEC-1B and Ishikawa cells. The results revealed that elevation of miR-545-3p remarkably reduced the luciferase activity of WT-FAM98A 3'UTR reporter but not MUT-FAM98A 3'UTR (**Fig. 5B and C**). In comparison to normal tissues, FAM98A mRNA and protein levels were markedly increased in ECa tissues (**Fig. 5D and E**). Furthermore, FAM98A mRNA level inversely correlated with miR-545-3p expression in ECa tissues (**Fig. S2B**). In addition, FAM98A protein level exhibited a prominent elevation in ECa cells (HEC-1B, EEC and Ishikawa) compared to normal hESCs (**Fig. 5F**). The ability of miR-545-3p in affecting FAM98A expression was validated. Western blot analysis showed that FAM98A protein expression was decreased by miR-545-3p overexpression and elevated by reduced miR-545-3p abundance (**Fig. 5G and H**). To sum up, these data suggested that miR-545-3p directly targeted and repressed FAM98A. In addition, circ-IFT80 silencing led to a striking reduction in the level of FAM98A protein, and co-transfection of anti-miR-545-
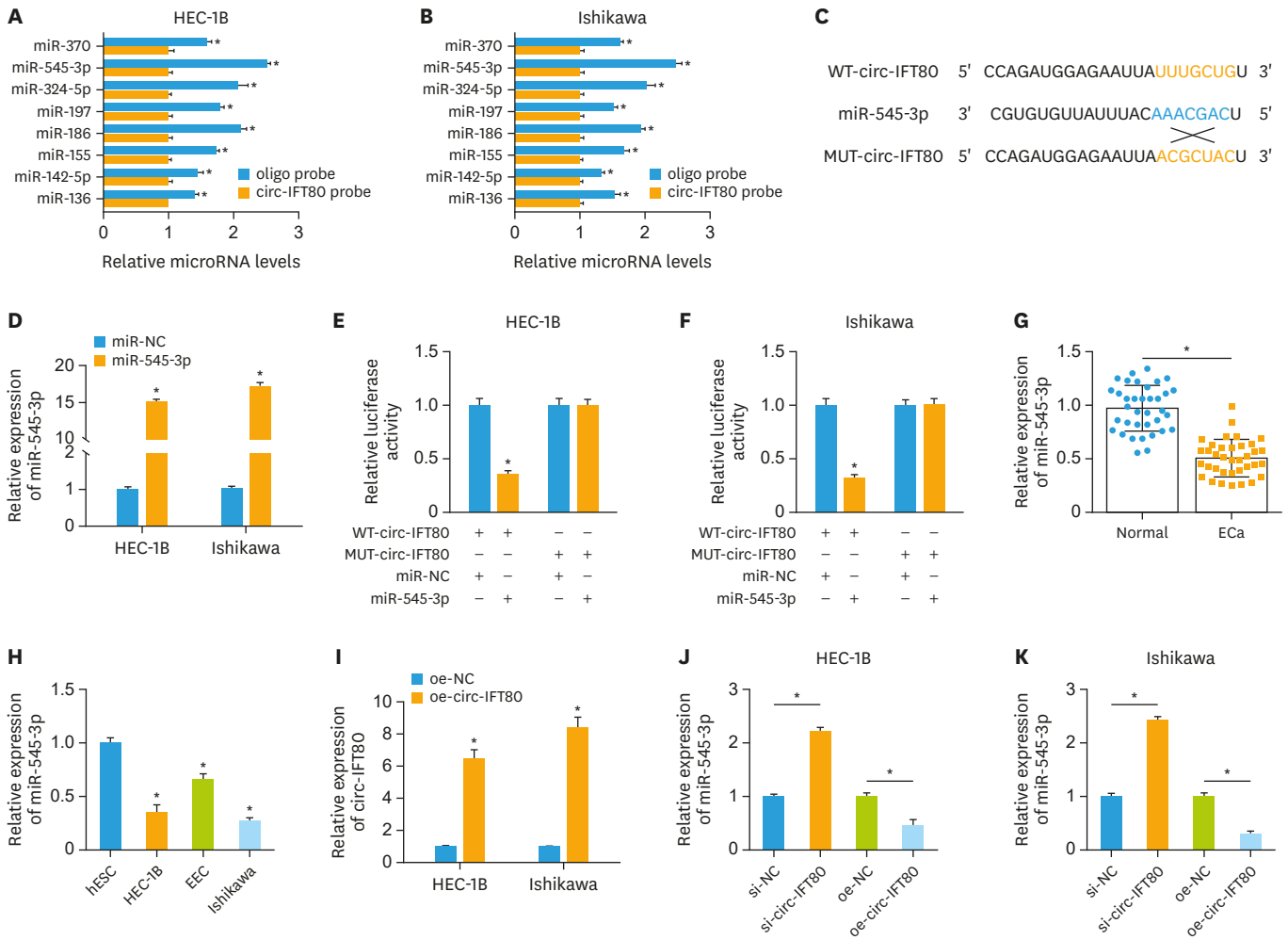
Fig. 4. Targeted regulation of circ-IFT80 and miR-545-3p. (A,B) RNA pull-down method was used to assess the relationship between circ-IFT80 and 8 candidate miRNAs. (C) The binding sequence between circ-IFT80 and miR-545-3p was displayed by circinteractome software. (D) The transfection efficiency of miR-545-3p mimics was detected using qRT-PCR. (E, F) The supposed targeting relationship was confirmed via dual-luciferase reporter assay. (G, H) miR-545-3p level in ECa tissues (n=35) and cells (HEC-1B, EEC and Ishikawa) was measured by qRT-PCR. (I) After introducing oe-NC or oe-circ-IFT80 into ECa cells, circ-IFT80 level was tested using qRT-PCR. (J, K) MiR-545-3p level was examined via qRT-PCR in HEC-1B and Ishikawa cells transfected with si-NC, si-circ-IFT80, oe-NC or oe-circ-IFT80. circ-IFT80, circular RNA intraflagellar transport 80; ECa, endometrial cancer; hESC, human embryonic stem cell; miR-545-3p, microRNA-545-3p; si-circ-IFT80, circular RNA intraflagellar transport 80 siRNA; qRT-PCR, quantitative real-time polymerase chain reaction.
$^*p<0.05$.

3p partly abrogated this effect (**Fig. 5I and J**). Overall, these results indicated that circ-IFT80 sequestered miR-545-3p to regulate FAM98A expression.

5. Circ-IFT80 regulates the malignant phenotypes of ECa cells by regulating miR-545-3p/FAM98A axis

To evaluate whether miR-545-3p is involved in the regulation of circ-IFT80, we reduced miR-545-3p expression in circ-IFT80-silenced cells. After transfection with anti-miR-545-3p, miR-545-3p level presented a marked decrease in HEC-1B and Ishikawa cells (**Fig. S4A**). Further functional experiments suggested that introduction of anti-miR-545-3p partially abolished circ-IFT80 deletion-driven suppression on cell proliferation (**Fig. S4B-D**), migration (**Fig. S4E**), invasion (**Fig. S4F**) and angiogenesis (**Fig. S4G**). Furthermore, down-regulation of miR-545-3p markedly attenuated circ-IFT80 silence-induced cell cycle arrest and cell apoptosis in HEC-1B and Ishikawa cells (**Fig. S5A-C**). Additionally, knockdown of miR-545-3p reversed
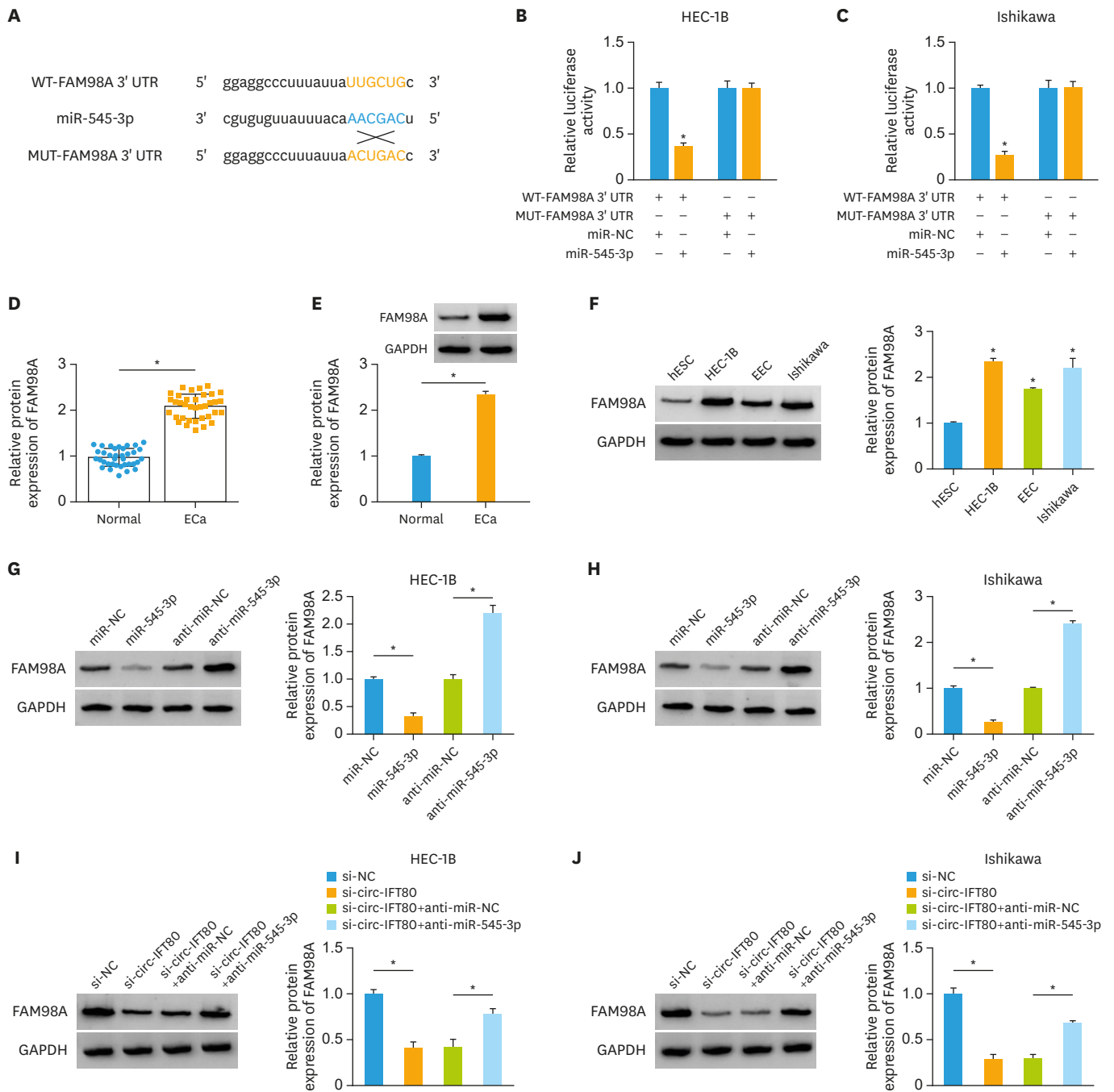
Fig. 5. Targeting association between miR-545-3p and FAM98A. (A-C) The possible targeting relationship between miR-545-3p and FAM98A was predicted through starBase software and verified via dual-luciferase reporter assay. (D, E) FAM98A mRNA and protein levels in ECa tissues (n=35) and matched normal tissues (n=35) were tested via qRT-PCR and Western blot. (F) FAM98A protein level in ECa cells (HEC-1B, EEC and Ishikawa) and hESC cells was measured using Western blot. (G, H) FAM98A protein level was detected by Western blot in HEC-1B and Ishikawa cells transfected with miR-NC, miR-545-3p, anti-miR-NC or anti-miR-545-3p. (I, J) The protein level of FAM98A in HEC-1B and Ishikawa cells transfected with si-circ-IFT80 or/and anti-miR-545-3p was examined by Western blot.
circ-IFT80, circular RNA intraflagellar transport 80; ECa, endometrial cancer; GAPDH, glyceraldehyde 3-phosphate dehydrogenase; hESC, human embryonic stem cell; miR-545-3p, microRNA-545-3p; qRT-PCR, quantitative real-time polymerase chain reaction; si-circ-IFT80, circular RNA intraflagellar transport 80 siRNA.
*$p < 0.05$.

the decrease in PCNA and Bcl-2 levels and the increase in Bax level caused by circ-IFT80 depletion (**Fig. S5D and E**).

To elucidate whether miR-545-3p targeted FAM98A to influence ECa development, functional experiments were performed in ECa cells by introducing miR-545-3p mimic or/and FAM98A overexpression vector. Introduction of FAM98A overexpression vector resulted in a significant up-regulation of FAM98A in ECa cells, as gauged by Western blot assay (**Fig. S6A**). In contrast to the control group, up-regulation of miR-545-3p hindered cell proliferation (**Fig. S6B-D**), migration (**Fig. S6E**), invasion (**Fig. S6F**) and tube formation (**Fig. S6G**), while these impacts were partially recovered by overexpression of FAM98A. Furthermore, elevation of FAM98A abolished the stimulating effect of miR-545-3p mimics on cycle arrest and apoptosis of ECa cells (**Fig. S7A-C**). Additionally, up-regulation of FAM98A counteracted the impacts of miR-545-3p overexpression on PCNA, Bcl-2 and Bax levels (**Fig. S7D and E**). Overall, these data demonstrated that circ-IFT80 knockdown inhibited the malignant behaviors of ECa cells by targeting miR-545-3p/FAM98A axis.

6. Circ-IFT80 depletion blocks tumor growth in vivo

We also investigated the role of circ-IFT80 in tumor growth in vivo by injecting Ishikawa cells coding sh-circ-IFT80 into mice. As shown in **Fig. 6A-C**, tumor volume and weight were markedly declined in the sh-circ-IFT80 group compared to the sh-NC group. Additionally, we examined the expression of related genes in the tumors, and the results revealed that sh-circ-IFT80 transfection resulted in a significant decrease in circ-IFT80 and FAM98A levels and a striking increase in miR-545-3p level (**Fig. 6D and E**). Moreover, IHC analysis suggested that silencing of circ-IFT80 reduced the cells staining with Ki67 (**Fig. 6F**). Altogether, these data indicated that circ-IFT80 knockdown hindered tumor growth in vivo.
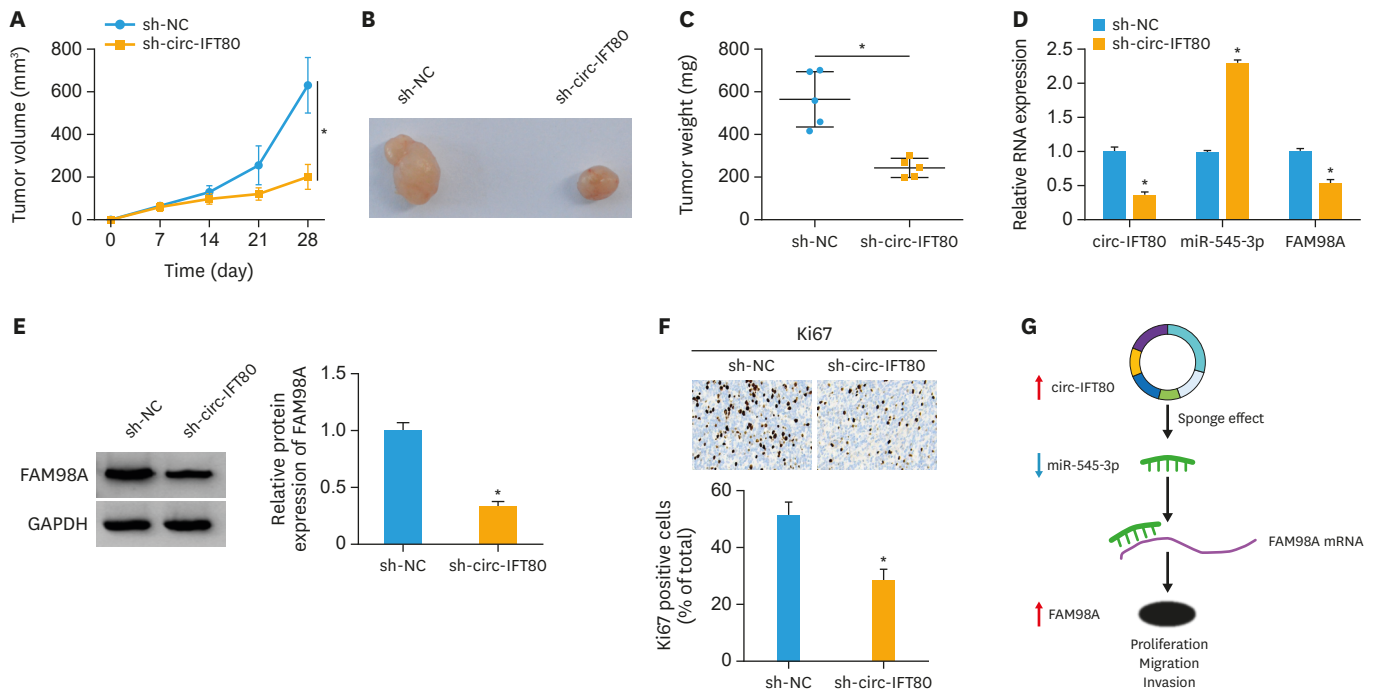

Fig. 6. Circ-IFT80 depletion blocks tumor growth in vivo. (A) After Ishikawa cells containing sh-circ-IFT80 or sh-NC were injected into mice, tumor growth curves were drawn (n=5 per group). (B, C) Following 28 days, xenograft tumors were excised and weighed (n=5 per group). (D, E) The levels of circ-IFT80, miR-545-3p and FAM98A in resected tumors were measured by qRT-PCR and Western blot (n=5 per group). (F) Ki67 positive cells were determined using IHC assay (n=5 per group). (G) Schematic diagram of the molecular mechanism of circ-IFT80/miR-545-3p/FAM98A axis in ECa cell progression.
circ-IFT80, circular RNA intraflagellar transport 80; ECa, endometrial cancer; GAPDH, glyceraldehyde 3-phosphate dehydrogenase; IHC, immunohistochemistry; miR-545-3p, microRNA-545-3p; qRT-PCR, quantitative real-time polymerase chain reaction.
*p<0.05.

DISCUSSION

In recent years, circRNAs have attracted more attention in RNA research due to their important roles in many diseases [21]. Increasing evidence has suggested that circRNAs exert crucial roles in ECa by participating in diverse biological processes [22]. A recent study uncovered that circ-IFT80 contributed to the progression of ECa via sequestering miR-324-5p and inducing HMGA1 [12]. Although this report unveiled a mechanism underlying circ-IFT80 regulation in ECa, our understanding of its molecular determinants is still limited. In this study, we focused on the ceRNA activity of circ-IFT80 in ECa. Using in vitro and in vivo experiments, we first uncovered the circ-IFT80/miR-545-3p/FAM89A ceRNA network in ECa (**Fig. 6G**).

The ceRNA hypothesis proposes that circRNAs can function as ceRNAs to bind to miRNAs, functionally liberating mRNAs targeted by that set of miRNAs [23,24]. For example, up-regulation of circWHSC1 promoted ECa cell proliferation, migration and invasiveness by inducing NPM1 through competitively binding to miR-646 [25]. Also, deficiency of circ_0061140 impeded the growth and metastasis of ECa by elevating miR-149-5p and decreasing STAT3 [26]. In this paper, we confirmed that circ-IFT80 was mainly present in the cytoplasm of ECa cells. Based on this, we speculated that circ-IFT80 might act as a ceRNA for miRNAs. Here we reported, for the first time, that circ-IFT80 targeted miR-545-3p. Some investigations have manifested the contradictory role of miR-545-3p in human cancers. For example, up-regulation of miR-545-3p facilitated tumor growth and metastasis by down-regulating metallothionein 1 M in hepatocellular carcinoma [27]. Conversely, miR-545-3p worked as a tumor inhibitor in epithelial ovarian carcinoma [28]. Moreover, Zhong et al. [20] uncovered that knockdown of miR-545-3p abrogated the repressive effect of AFAP-AS1 deficiency on the angiogenesis and invasiveness of ECa via controlling VEGFA expression. In the present research, we were the first to unveil that miR-545-3p was responsible for the regulation of circ-IFT80 in ECa.

FAM98A is a novel substrate for PRMT1, which is a potential oncogenic protein [29]. In colorectal carcinoma, depletion of FAM98A restrained the malignant progression of tumor cells [30]. In lung carcinoma, FAM98A up-regulation enhanced tumor cell growth by inducing the P38-ATF2 pathway [31]. Li et al. [32] suggested that FAM98A level was prominently elevated in ECa, which was in agreement with our findings. In this paper, we first identified FAM98A as a direct and functional target of miR-545-3p in ECa cells. Furthermore, we first uncovered that circ-IFT80 acted as a ceRNA to induce FAM98A expression by competing for shared miR-545-3p.

In summary, we demonstrated a novel ceRNA network, circ-IFT80/miR-545-3p/FAM89A axis, in regulating ECa cell behaviors. Our findings provided a novel insight into the pathogenesis of ECa and revealed promising therapeutic targets.

SUPPLEMENTARY MATERIALS

Table S1
Correlation between circ-IFT80 expression and clinical features in endometrial cancer patients (n=35)

Click here to view

Table S2

Correlation between miR-545-3p expression and clinical features in endometrial cancer patients (n=35)

Click here to view

Fig. S1

Effects of circ-IFT80 overexpression on cell proliferation, migration and invasion. hESC cells were transfected with oe-NC control or oe-circ-IFT80 and checked for circ-IFT80 expression by qRT-PCR (A), cell proliferation by EdU assay (B), cell migration (C) and invasion (D) by transwell assay.

Click here to view

Fig. S2

Expression correlation of miR-545-3p and circ-IFT80 (A) or FAM98A (B) in ECa tissues using Pearson's correlation coefficients.

Click here to view

Fig. S3

Selection of FAM98A. The expression levels of 6 genes were assessed by qRT-PCR in HEC-1B (A) and Ishikawa (B) cells transfected with miR-NC mimic or miR-545-3p mimic.

Click here to view

Fig. S4

Silence of circ-IFT80 inhibits the malignant phenotypes of ECa cells by miR-545-3p. (A) The transfection efficiency of miR-545-3p inhibitor was validated via qRT-PCR. Following introducing si-circ-IFT80 or/and anti-miR-545-3p into HEC-1B and Ishikawa cells, cell proliferation ability (B, C), EdU positive cells (D), cell migration and invasion capabilities (E, F), and angiogenesis (G) were evaluated via CCK-8, EdU, transwell and tube formation.

Click here to view

Fig. S5

Silence of circ-IFT80 enhances cell cycle progression and apoptosis by miR-545-3p. Following introducing si-circ-IFT80 or/and anti-miR-545-3p into HEC-1B and Ishikawa cells, cell cycle distribution (A, B) and apoptosis (C) were evaluated by flow cytometry. (D, E) The relevant protein levels were determined using Western blot.

Click here to view

Fig. S6

MiR-545-3p hinders the malignant progression of ECa cells via regulating FAM98A. (A) The overexpression efficiency of FAM98A was tested using Western blot. After transfecting miR-545-3p or/and FAM98A into HEC-1B and Ishikawa cells, cell proliferation capacity (B, C),

EdU positive cells (D), cell migration and invasion abilities (E, F), and angiogenesis (G) were assessed via CCK-8, EdU, transwell and tube formation.

Click here to view

Fig. S7

MiR-545-3p impedes cell cycle progression and apoptosis via regulating FAM98A. After transfecting miR-545-3p or/and FAM98A into HEC-1B and Ishikawa cells, cell cycle distribution (A, B) and apoptosis (C) were evaluated by flow cytometry. (D, E) The relevant protein levels were determined using Western blot.

Click here to view

REFERENCES

1. Brooks RA, Fleming GF, Lastra RR, Lee NK, Moroney JW, Son CH, et al. Current recommendations and recent progress in endometrial cancer. CA Cancer J Clin 2019;69:258-79.
   PUBMED | **CROSSREF**

2. Sung H, Ferlay J, Siegel RL, Laversanne M, Soerjomataram I, Jemal A, et al. Global cancer statistics 2020: GLOBOCAN estimates of incidence and mortality worldwide for 36 cancers in 185 countries. CA Cancer J Clin 2021;71:209-49.
   PUBMED | **CROSSREF**

3. Post CCB, Westermann AM, Bosse T, Creutzberg CL, Kroep JR. PARP and PD-1/PD-L1 checkpoint inhibition in recurrent or metastatic endometrial cancer. Crit Rev Oncol Hematol 2020;152:102973.
   PUBMED | **CROSSREF**

4. Li J, Sun D, Pu W, Wang J, Peng Y. Circular RNAs in cancer: biogenesis, function, and clinical significance. Trends Cancer 2020;6:319-36.
   PUBMED | **CROSSREF**

5. Tang X, Ren H, Guo M, Qian J, Yang Y, Gu C. Review on circular RNAs and new insights into their roles in cancer. Comput Struct Biotechnol J 2021;19:910-28.
   PUBMED | **CROSSREF**

6. Sun Q, Qi X, Zhang W, Li X. Knockdown of circRNA_0007534 suppresses the tumorigenesis of cervical cancer via miR-206/GREM1 axis. Cancer Cell Int 2021;21:54.
   PUBMED | **CROSSREF**

7. Hou W, Zhang Y. Circ_0025033 promotes the progression of ovarian cancer by activating the expression of LSM4 via targeting miR-184. Pathol Res Pract 2021;217:153275.
   PUBMED | **CROSSREF**

8. Ye F, Tang QL, Ma F, Cai L, Chen M, Ran XX, et al. Analysis of the circular RNA transcriptome in the grade 3 endometrial cancer. Cancer Manag Res 2019;11:6215-27.
   PUBMED | **CROSSREF**

9. Guo J, Tong J, Zheng J. Circular RNAs: a promising biomarker for endometrial cancer. Cancer Manag Res 2021;13:1651-65.
   PUBMED | **CROSSREF**

10. Shen Q, He T, Yuan H. Hsa_circ_0002577 promotes endometrial carcinoma progression via regulating miR-197/CTNND1 axis and activating Wnt/β-catenin pathway. Cell Cycle 2019;18:1229-40.
    PUBMED | **CROSSREF**

11. Jia Y, Liu M, Wang S. CircRNA hsa_circRNA_0001776 inhibits proliferation and promotes apoptosis in endometrial cancer via downregulating LRIG2 by sponging miR-182. Cancer Cell Int 2020;20:412.
    PUBMED | **CROSSREF**

12. Liu Y, Chang Y, Cai Y. Circ_0067835 sponges miR-324-5p to induce HMGA1 expression in endometrial carcinoma cells. J Cell Mol Med 2020;24:13927-37.
    PUBMED | **CROSSREF**

13. Panda AC. Circular RNAs act as miRNA sponges. Adv Exp Med Biol 2018;1087:67-79.
    PUBMED | **CROSSREF**

14. Huang A, Zheng H, Wu Z, Chen M, Huang Y. Circular RNA-protein interactions: functions, mechanisms, and identification. Theranostics 2020;10:3503-17.
PUBMED | **CROSSREF**

15. Shi Y, Jia L, Wen H. Circ_0109046 promotes the progression of endometrial cancer via regulating miR-136/HMGA2 axis. Cancer Manag Res 2020;12:10993-1003.
PUBMED | **CROSSREF**

16. Yanokura M, Banno K, Iida M, Irie H, Umene K, Masuda K, et al. MicroRNAS in endometrial cancer: recent advances and potential clinical applications. EXCLI J 2015;14:190-8.
PUBMED

17. Vasilatou D, Sioulas VD, Pappa V, Papageorgiou SG, Vlahos NF. The role of miRNAs in endometrial cancer. Epigenomics 2015;7:951-9.
PUBMED | **CROSSREF**

18. Xu JB. MicroRNA-93-5p/IFNAR1 axis accelerates metastasis of endometrial carcinoma by activating the STAT3 pathway. Eur Rev Med Pharmacol Sci 2019;23:5657-66.
PUBMED | **CROSSREF**

19. Tian Y, Chen YY, Han AL. MiR-1271 inhibits cell proliferation and metastasis by targeting LDHA in endometrial cancer. Eur Rev Med Pharmacol Sci 2019;23:5648-56.
PUBMED | **CROSSREF**

20. Zhong Y, Wang Y, Dang H, Wu X. LncRNA AFAP1-AS1 contributes to the progression of endometrial carcinoma by regulating miR-545-3p/VEGFA pathway. Mol Cell Probes 2020;53:101606.
PUBMED | **CROSSREF**

21. Li HM, Ma XL, Li HG. Intriguing circles: conflicts and controversies in circular RNA research. Wiley Interdiscip Rev RNA 2019;10:e1538.
PUBMED | **CROSSREF**

22. Dong P, Xu D, Xiong Y, Yue J, Ihira K, Konno Y, et al. The expression, functions and mechanisms of circular RNAs in gynecological cancers. Cancers (Basel) 2020;12:1472.
PUBMED | **CROSSREF**

23. Cui X, Wang J, Guo Z, Li M, Li M, Liu S, et al. Emerging function and potential diagnostic value of circular RNAs in cancer. Mol Cancer 2018;17:123.
PUBMED | **CROSSREF**

24. Salafia A, Kharkar RD. Thalidomide and exfoliative dermatitis. Int J Lepr Other Mycobact Dis 1988;56:625.
PUBMED

25. Liu Y, Chen S, Zong ZH, Guan X, Zhao Y. CircRNA WHSC1 targets the miR-646/NPM1 pathway to promote the development of endometrial cancer. J Cell Mol Med 2020;24:6898-907.
PUBMED | **CROSSREF**

26. Liu Y, Chang Y, Cai Y. Hsa_circ_0061140 promotes endometrial carcinoma progression via regulating miR-149-5p/STAT3. Gene 2020;745:144625.
PUBMED | **CROSSREF**

27. Changjun L, Feizhou H, Dezhen P, Zhao L, Xianhai M. MiR-545-3p/MT1M axis regulates cell proliferation, invasion and migration in hepatocellular carcinoma. Biomed Pharmacother 2018;108:347-54.
PUBMED | **CROSSREF**

28. Shi J, Xu X, Zhang D, Zhang J, Yang H, Li C, et al. Long non-coding RNA PTPRG-AS1 promotes cell tumorigenicity in epithelial ovarian cancer by decoying microRNA-545-3p and consequently enhancing HDAC4 expression. J Ovarian Res 2020;13:127.
PUBMED | **CROSSREF**

29. Akter KA, Mansour MA, Hyodo T, Ito S, Hamaguchi M, Senga T. FAM98A is a novel substrate of PRMT1 required for tumor cell migration, invasion, and colony formation. Tumour Biol 2016;37:4531-9.
PUBMED | **CROSSREF**

30. Akter KA, Mansour MA, Hyodo T, Senga T. FAM98A associates with DDX1-C14orf166-FAM98B in a novel complex involved in colorectal cancer progression. Int J Biochem Cell Biol 2017;84:1-13.
PUBMED | **CROSSREF**

31. Zheng R, Liu Q, Wang T, Wang L, Zhang Y. FAM98A promotes proliferation of non-small cell lung cancer cells via the P38-ATF2 signaling pathway. Cancer Manag Res 2018;10:2269-78.
PUBMED | **CROSSREF**

32. Li Z, Li N, Sun X, Wang J. FAM98A promotes cancer progression in endometrial carcinoma. Mol Cell Biochem 2019;459:131-9.
PUBMED | **CROSSREF**